Geomagnetic and Ionospheric Disturbances During Moderate Seismic Events in South America

S.A.Sánchez,[1] E.A. Kherani [1], V. Klausner[2], E.R.de Paula [1], F.C.De Meneses[3] (1)National Institute for Space Research (INPE); (2)Universidade do Vale do Paraíba (UNIVAP); (3)Universidad Autónoma de Nuevo León (UANL).

Introduction

Seismic-Atmospheric Ionospheric Disturbances (SAIDs) can be generated by seismic activity. Earth displacement due to earthquakes (EQ) causes effects on the atmosphere up to 300 km in height, as a result of the coupling of the Lithosphere Atmosphere Ionosphere interfaces. For the moderate EQ (Mw=6.3) using GPS receiver data, we detect the SAIDs that are associated with gravity waves with velocities 0.22 and 0.16 km/s. For EQ (Mw=7.1) using magnetometer networks, we detect SAIDs in the form of geomagnetic disturbances that have propagation velocities greater than the velocity of the primary and secondary waves recorded by seismographs, and due to the very high velocities, these disturbances may be associated mainly to the shear or oblique Alfvén waves.

Method

In this work two methods will be used to calculate the SAIDs with data from the Magnetometers: Hilbert Huang Transform (HHT) techniques (HUANG et al, 1998) and Continuous Wavelet Transform (CWT) (CHAN, 1995). These techniques are widely used to decompose signals.

And to use data from GPS stations, the Bandpass filter is used. The TEC shown in Figure 5 is derived from the following definition:
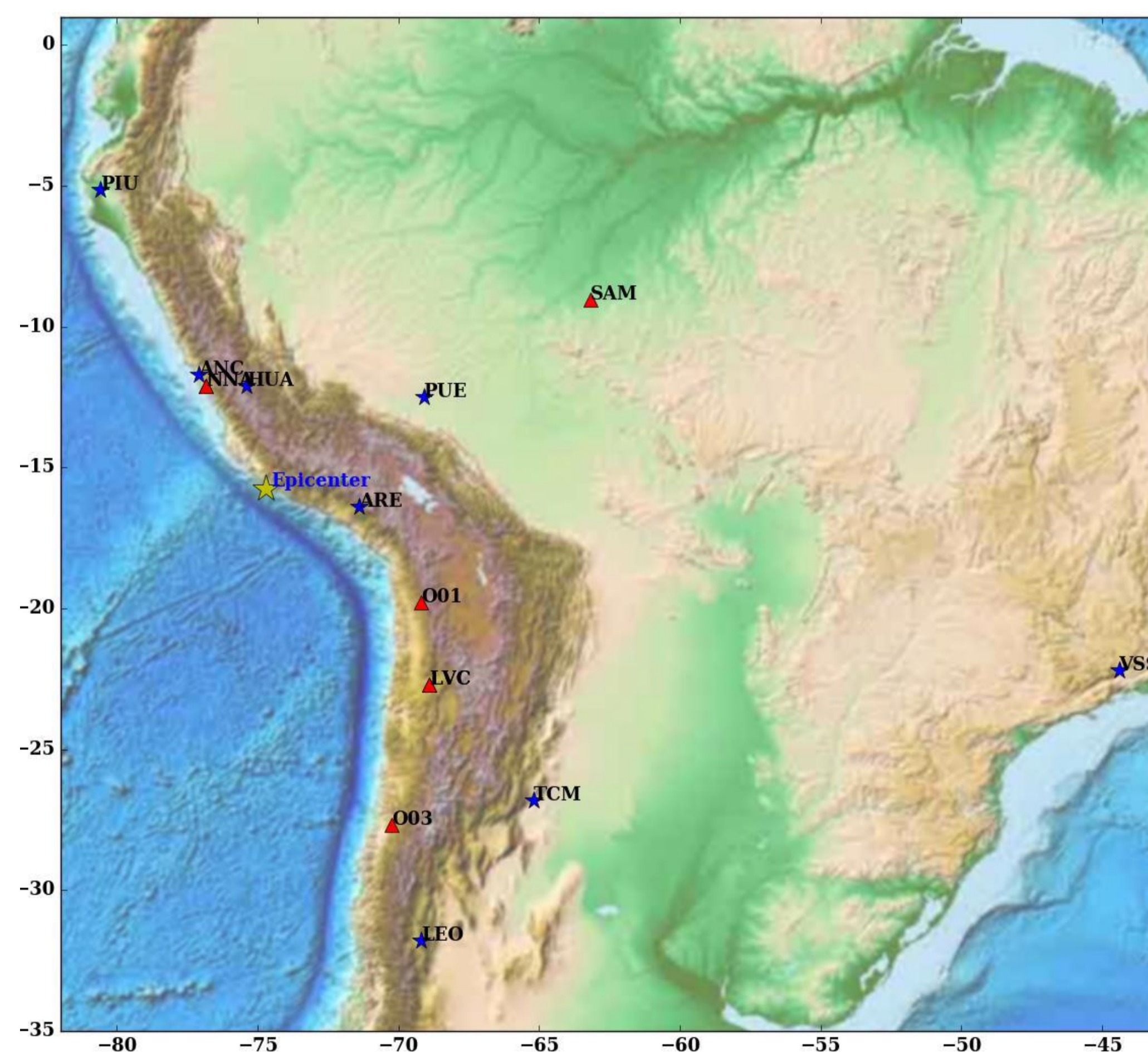
$$TEC_{combi} = TEC_{phase} - < TEC_{phase} - TEC_{pseudo} >$$

where

$$TEC_{phase} = 9.52(\lambda_2\Phi_2 - \lambda_1\Phi_1); TEC_{pseudo} = 9.52(P_2 - P_1)$$

Subscripts 1 and 2 represent the measurements in the L1 = 1575.42 MHz e L2 = 1227.60 MHz frequencies, Φ and P are the pseudo distance and phase measurements, $\lambda_1 = 0.19$ m, $\lambda_2 = 0.24$ m are the wavelengths of L1 and L2

Results with Magnetometers from the EQ 7.1 of 01/14/18

Fig.1 Map with the location of the seismic and geomagnetic stations. Where the yellow star represents the epicenter of the EQ, the red triangles represent the seismic stations and the blue stars represent the geomagnetic stations.

In Figure 2, following the technique proposed by Utada et al. (2011), a subtraction is made between the horizontal component data of each station and the data from the most distant geomagnetic station (VSS). This method is very important to remove possible external magnetic contributions that might affect our analysis.
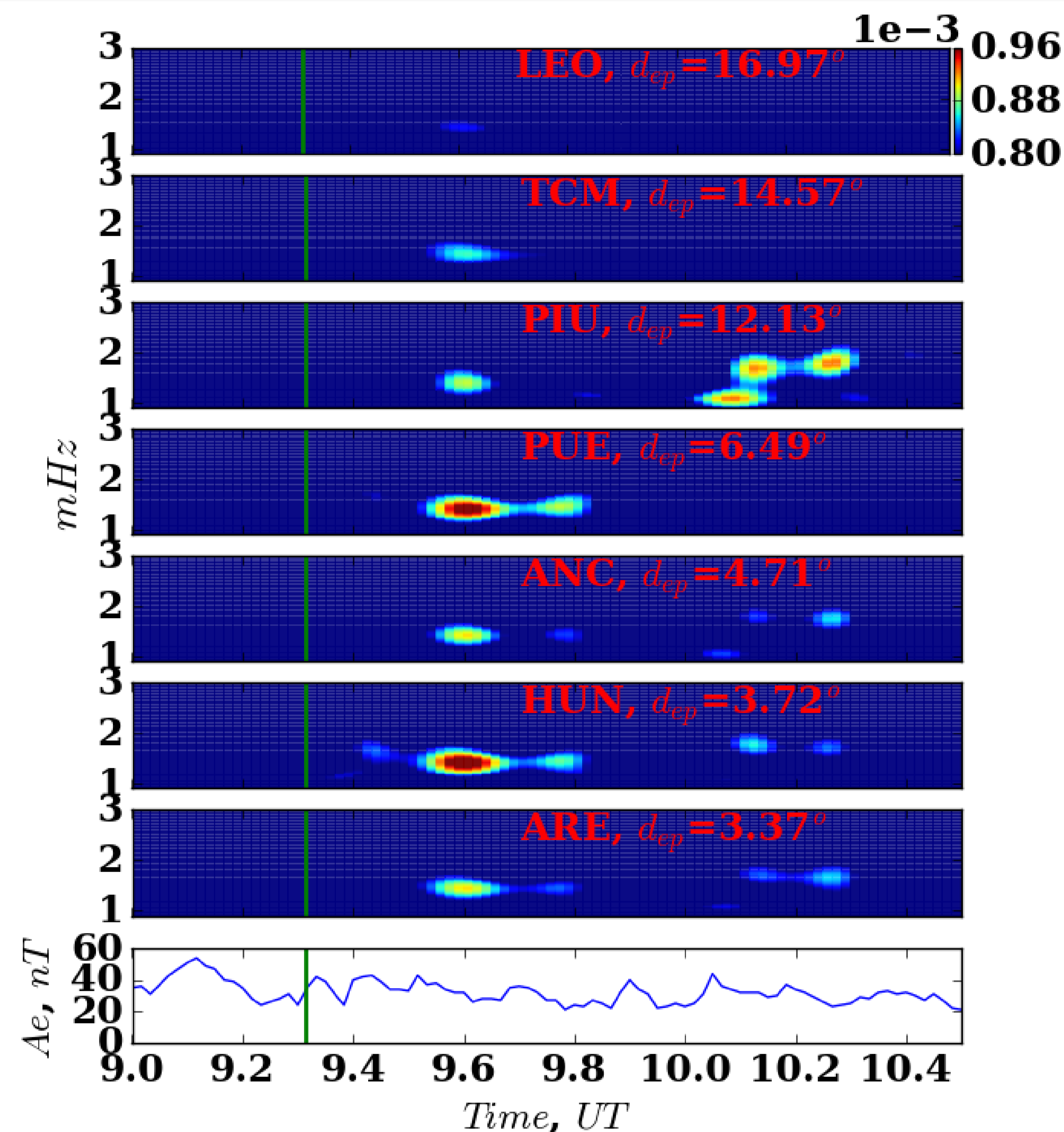

Fig.2 Spectral analysis of the horizontal component of the magnetic field measured by magnetometer. The green vertical line represents the EQ time. A clear increase in spectral density by 9.6 UT is observed about 18 minutes after the EQ.

Disturbance propagation analysis in Figure 3 was developed with the HHT method.
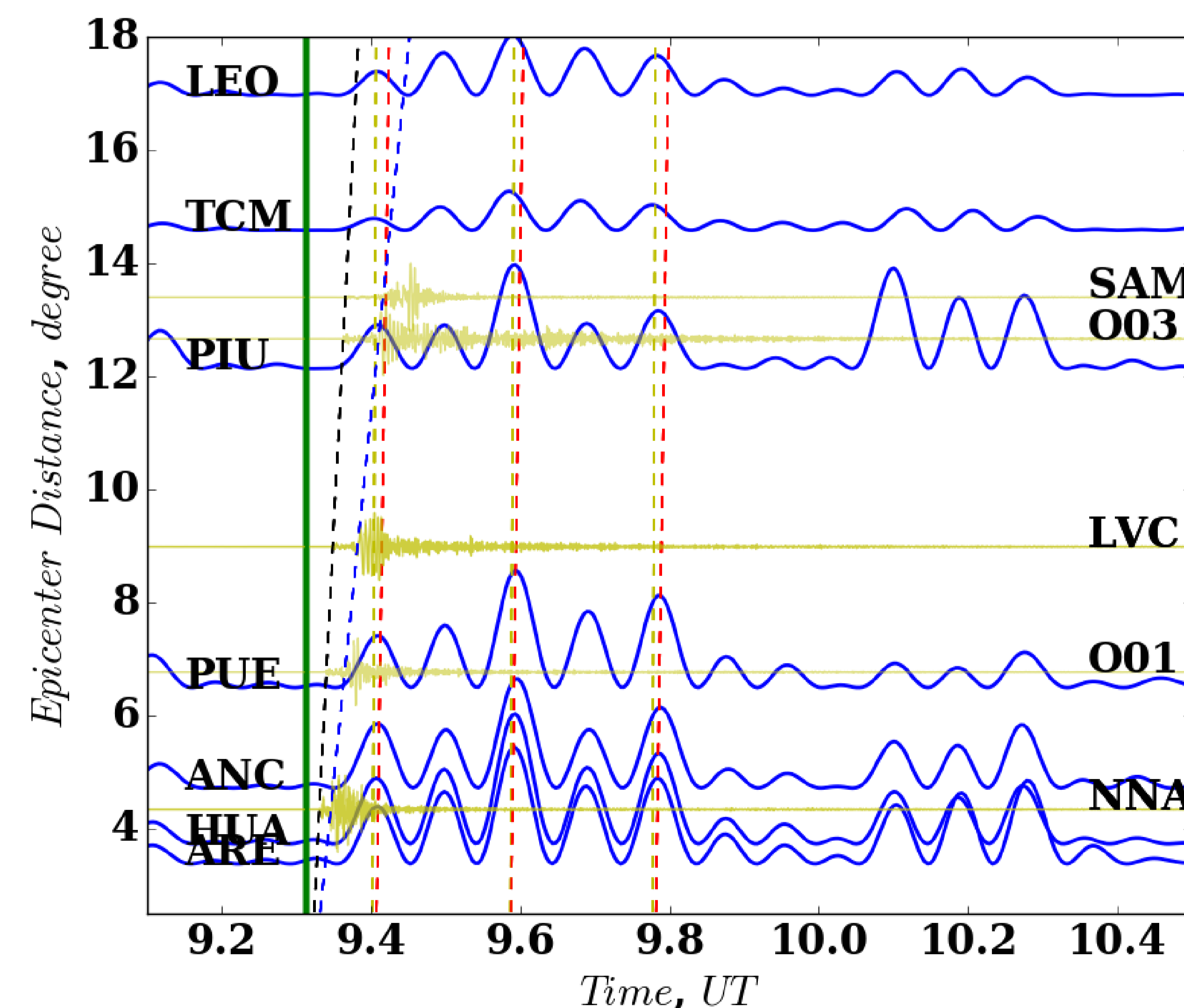
Fig.3 The blue lines show the displacement of the waves, and the red dotted lines are traces to calculate the speed and the period of the wave recorded by the magnetometers. The disturbances shown in yellow are recorded by local seismographs, the black and blue dotted lines show the P (primary seismic longitudinal waves propagating in the ground) and S (transverse second waves in the ground) velocities respectively

Results with GPS from the EQ 6.3 of 01/21/18
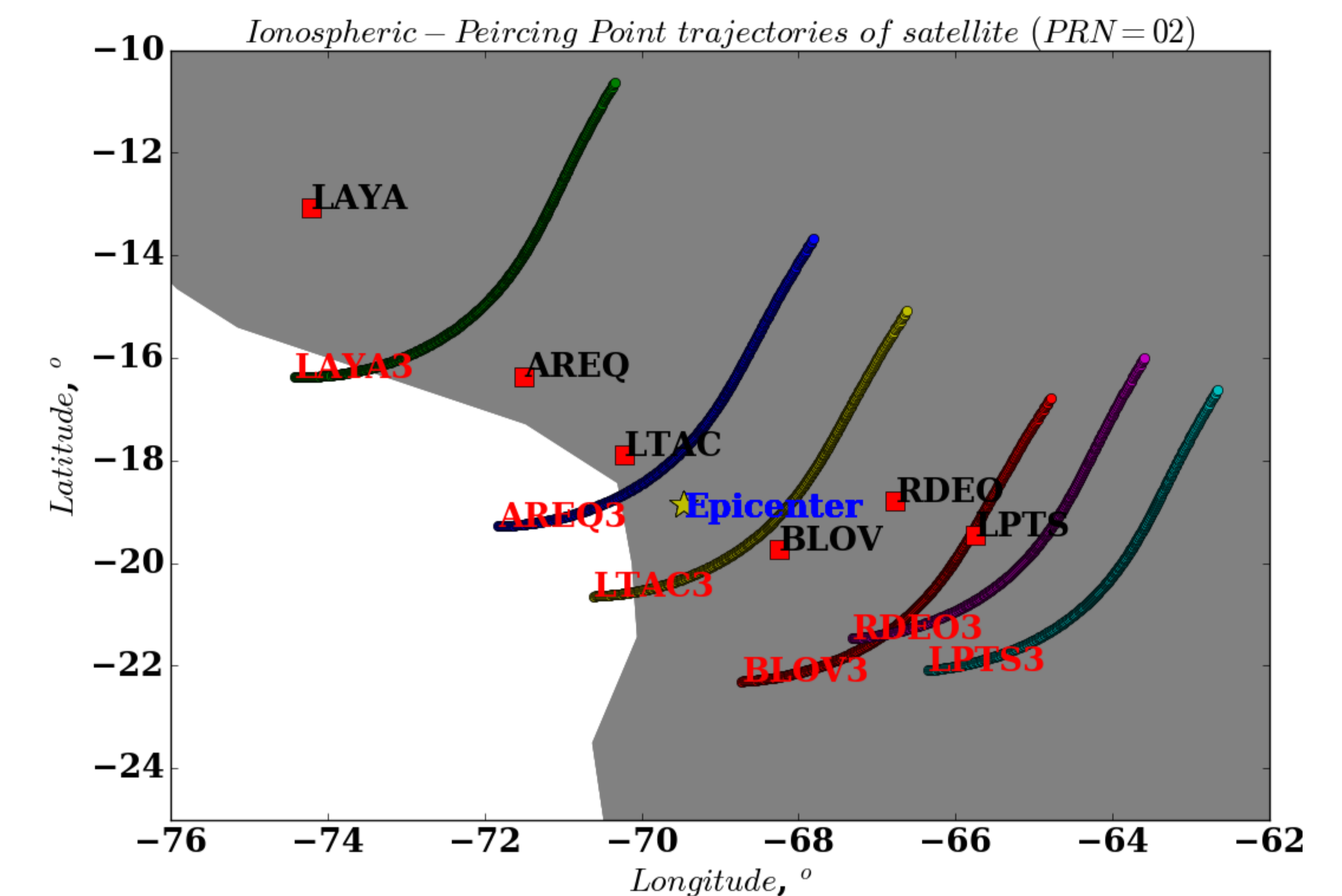
Fig.4 Location of the GPS stations and trajectories of the IPPs used to study the EQ. Where yellow star represents the epicenter of the EQ, the red squares represent the GPS stations and the colored lines represent the trajectories of the IPPs, from 1.00 hour to 4.5 hours.
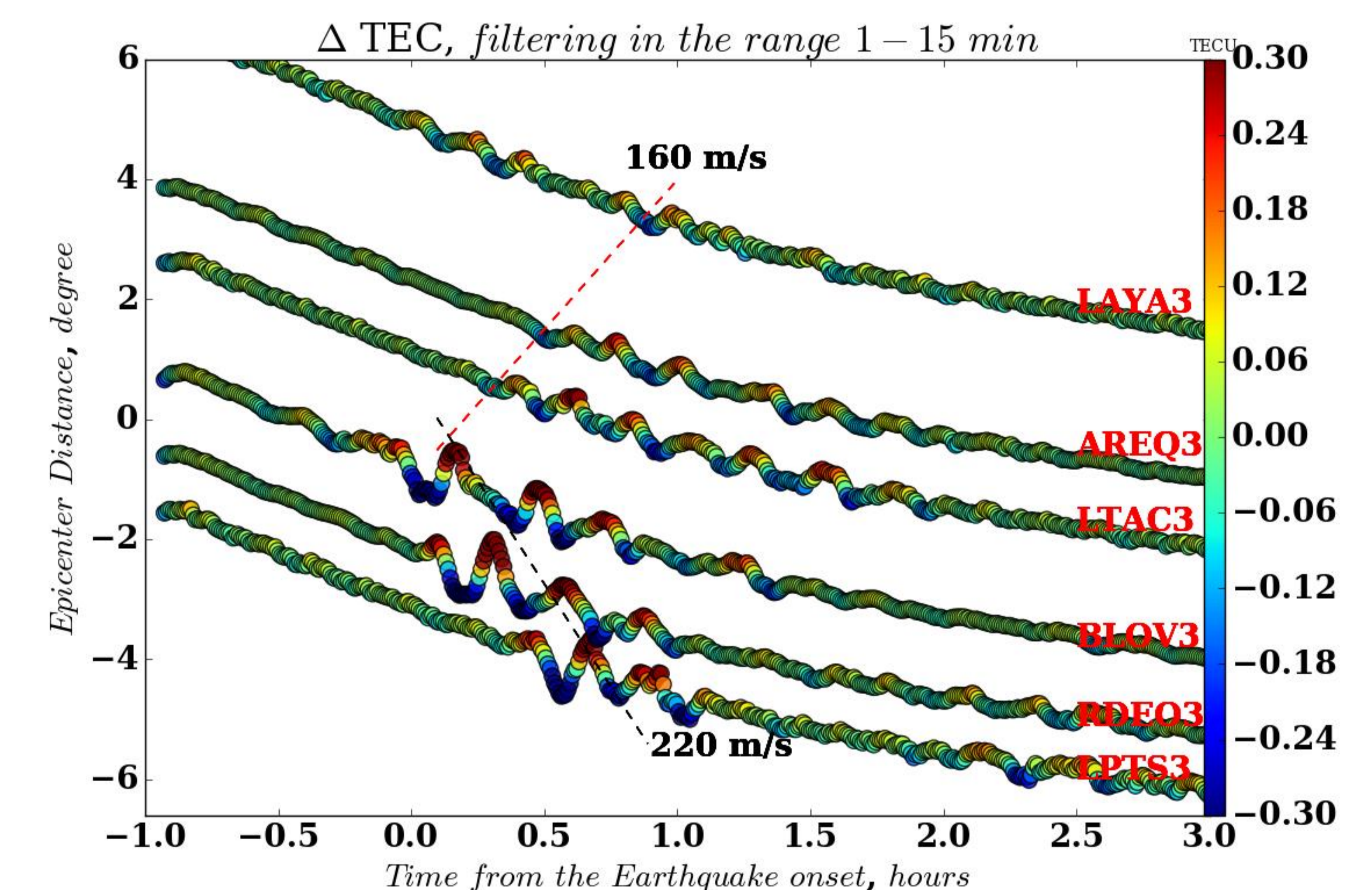
Fig. 5 Shows propagation of TIDs, with GPS data PRN 03

Conclusions

Data analysis with HHT and CWT time series and electromagnetic wave propagation in geomagnetic field data, for Mw=7.1 earthquake, shows clearly detectable SAIDs. Using the GPS receiver network, for the magnitude Mw=6.3 we detected the SAIDs associated with gravity waves and velocities (220 and 160 m/s), and a favorable preconditioning offered by the original non-seismic MSTIDs reinforce the seismic contribution rise to the detectable level.

Reference.

HUANG, E.; SHEN, Z.; LONG, S.; WU, M.; SHIH, H.; ZHENG, Q.; YEN, N.; TUNG, C.; LIU, H. H. The empirical mode decomposition and the hilbert spectrum for nonlinear and non-stationary time series analysis. The Royal Society of London, 998.
CHAN, Y. T. wavelet Basics . [S.I.]: Kluwer Academic Publishers, 1995.
UTADA, H.; SHIMIZU, H.; OGAWA, T.; MAEDA, T.; FURUMURA, T.; YAMAMOTO, T.; YAMAZAKI, N.; YOSHITAKE, Y.; NAGAMACHI, S. Geomagnetic field changes in response to the 2011 off the pacific coast of tohoku earthquake and tsunami. Earth and Planetary Science Letters, v. 311, p. 11–27, 2011.